JOURNAL OF MATERIALS SCIENCE **40** (2005) 2141–2147

Material surfaces and nanosystems close to the melting temperature

U. TARTAGLINO, T. ZYKOVA-TIMAN
International School for Advanced Studies (SISSA-ISAS), via Beirut 2, 34014 Trieste, Italy; INFM Democritos National Simulation Center, Trieste, Italy

F. ERCOLESSI
Dipartimento di Fisica, Università di Udine, Via delle Scienze, 208, I-33100 Udine, Italy; INFM Democritos National Simulation Center, Trieste, Italy

E. TOSATTI
International School for Advanced Studies (SISSA-ISAS), via Beirut 2, 34014 Trieste, Italy; INFM Democritos National Simulation Center, Trieste, Italy; International Center for Theoretical Physics (ICTP), Strada Costiera 11, 34014, Trieste, Italy

This is a concise review of some facts and theory work on the equilibrium behavior of solid surfaces and nanosystems close to the bulk melting point. We focus in particular on computer simulation results obtained for metals and ionic insulators.

1. Surface melting and non-melting: Thermodynamics

A peculiar feature of the melting transition is the absence of a full hysteresis loop: while it is generally possible to supercool a liquid below the melting temperature T_m, it is usually difficult or impossible to overheat a solid above T_m. This suggests that a germ of the liquid phase is already present when T_m is approached from below, ready to propagate to the whole material. The most likely place where this germ could reside is the surface. This idea, proven to be correct, supplied the starting motivation for microscopic studies of surface melting (SM).

One of the first microscopic characterizations of SM is the famous medium-energy ion scattering experiment by Frenken and Van der Veen [1], showing the presence of a liquid film between crystal and vapor on the Pb(110) surface, whose thickness $\ell(T)$ increases rapidly to ∞ as T approaches T_m. A number of case studies are now known in the literature, and SM turns out to be generic for most crystal surfaces. It is however not general, and there are surfaces that do not melt at all, remains solid and crystalline all the way up to T_m. This behavior, alternative to SM, has been called surface nonmelting (NM) [2]. SM and NM can both occur for the same substance, of course on different crystallographic faces. For example NM was demonstrated for Pb(111) [3], while by contrast SM prevails on Pb(110).

In the language of wetting, SM is nothing else than complete wetting of the solid by *its own melt*. It takes place whenever the solid surface (more precisely the solid-vapor interface, SV) can lower its free energy by transforming into a sequence of two separate solid-liquid (SL) plus liquid-vapor (LV) interfaces, namely when the solid-vapor (SV) stability criterion $\gamma_{SV} < \gamma_{SL} + \gamma_{LV}$ is violated (where γ denotes the surface free energy) [4]. However, the "liquid" film may be only a few atomic layers thick, and one should allow for "interaction" effects between the SL and LV interfaces mediated by this thin film. The total Gibbs free energy change caused by melting a thickness ℓ can therefore be written as

$$\Delta G/A = [(\gamma_{SL} + \gamma_{LV}) - \gamma_{SV}] + \ell L \rho_L (T_m - T) + V(\ell) \quad (1)$$

where A is the surface area, L is the latent heat of melting per unit mass, ρ_L is the density of the liquid, and $V(\ell)$ represents a phenomenological SL-LV interface interaction term, which vanishes for $\ell \to \infty$ and tends to the positive value $V(0) = \gamma_{SV} - (\gamma_{SL} + \gamma_{LV})$ when $\ell \to 0$ (where ΔG should vanish by definition). SM replaces the SV interface with the two SL, LV interfaces, and this occurs when $V(\ell)$ is a globally *repulsive* interaction.

By contrast, NM corresponds to partial wetting, namely $\gamma_{SV} < \gamma_{SL} + \gamma_{LV}$ is fulfilled. Equation 1 still holds, with the same limits for $V(\ell)$ when $\ell \to 0$ and $\ell \to \infty$ given above, but now $V(0)$ is negative and the interface interaction is globally *attractive*. A useful mnemonic is that SL-LV repulsion causes the liquid film to expand (SM), while SL-LV attraction causes the liquid film to collapse and disappear (NM).

The microscopic mechanism behind interface attraction or repulsion varies, and may be eventually related to such different physical causes as layering [5], surface entropy [6] or Van der Waals forces [7]. The latter mechanism is very general and can actually be

described using the following macroscopic concepts. When two semi-infinite media are separated by a film of another medium with a finite thickness ℓ—the liquid phase between solid and vapor in our case—the interaction free energy between the two interfaces gets an asymptotical tail $V(\ell) \sim H/\ell^2$ due to the long range dispersion forces. If the optical density of the film is intermediate between that of the surrounding media, its so-called Hamaker constant H is positive, otherwise it is negative [8]. Positive H means a long range repulsion between the interfaces, which favors SM. That is generally the case for most metals and other materials, where the liquid is indeed less dense and a worse conductor than the solid. In some cases, such as in valence semiconductors and semimetals, melting leads to a denser (and generally metallic) liquid state, causing $H < 0$. Negative volume expansion at melting and a negative Hamaker constant occur also in other notable cases, among which water [9]. $H < 0$ implies a long range attraction between interfaces, and that hinders SM. In such cases, surfaces may even begin to wet close to T_m, but the growth of the wetting film is blocked, its thickness ℓ remaining microscopically thin at T_m.

In the remainder of this short review, we will focus primarily on materials of interest to the high temperature capillarity community, namely ionic insulators and metals. Readers are addressed to a more extensive review containing a larger selection of systems and physical issues, currently in preparation [10].

2. Theory

Several accurate theoretical frameworks to study SM have been developed. Due to space constraints, we will not discuss them here. We shall restrict ourselves to the simplest heuristic theory, and to computer simulations. Early crude but appealing reasoning leading to SM has indeed been based on heuristics. Bulk melting usually correlates well with the so called Lindemann melting criterion: when the r.m.s. thermal vibration amplitude of a solid reaches some 10% of the lattice spacing, the solid generally melts. Atoms at surfaces are less coordinated and generally looser than in bulk, and their vibration amplitudes are correspondingly larger. Surfaces will thus reach the Lindemann instability at a lower temperature than the bulk. Mechanical instability of the crystal is of course different from melting, which occurs at the free energy crossing of the solid and liquid phases, necessarily at a lower temperature than the instability. The Lindemann criterion can nonetheless heuristically be taken as a signal of the tendency to melt, and early bulk models were developed along these lines [11]. In the model semi-infinite solid (describing the surface), it is found that the mechanical instability of the first surface layer occurs at a temperature which is only about 3/4 that of the bulk [12]—a fact that had been long known and noted by precursors as Tammann and Stranski [13]. Self-consistent surface phonon calculations [14] and also experiments [15] later revealed that a precocious surface instability may be due to a more pronounced anharmonic outward expansion of the first surface layer relative to that in the bulk. Subsequent theoretical work, not further discussed here, presents a much more convincing and accurate picture of SM [16–18]

3. Simulations: Molecular dynamics

Atomistic Monte Carlo and Molecular Dynamics (MD) simulations of melting and surface melting constitute two very important tools in the field. Simulations may in many ways replace experiment, and must be similarly regarded and understood by means of theory. Similar to experiment, simulations often uncover novel or unexpected behavior. We shall concentrate on MD simulation and specifically on work done in our group. SM simulations are generally conducted on crystal slabs, made up of a sufficiently large number of atomic solid layers, with two free surfaces, or with one free and one "frozen" surface. The in-plane simulation cell size must be allowed to expand gradually as temperature increases, according to the bulk thermal expansion coefficient, to guarantee that the stress of the bulk-like part of the sample remains as close as possible to zero. MD consists of solving Newton's equations of motion, where forces are obtained as gradients with respect to atomic coordinates of a potential energy function $E_{pot}(\{\mathbf{R}\})$. Depending on systems, and on the accuracy needed, E_{pot} can be given either by empirical interatomic potentials or by first principles total energy calculations. Empirical two-body potentials, such as Lennard-Jones (LJ), or Born-Mayer-Huggins potentials, are not unreasonable for rare gas solids or for ionic crystals. Empirical *many body* potentials, such as the Embedded Atom Model [19], the glue model [20], the Finnis-Sinclair potential [21], etc., are much more suitable than two-body forces for metals. Many-body empirical potentials were developed also for such systems as valence semiconductors [22, 23], but here the first principles approach is generally more appropriate [24]. Typical SM simulation outputs are shown in Fig. 1 for a modified LJ system and for a metal surface respectively. Pictures for LJ(111), LJ(110) and Au(110), surfaces that undergo SM, illustrate the formation of a surface liquid film just below T_m. The configuration shown for Au(111), a NM surface, is not a stable one below T_m, and will evolve to a complete recrystallization. Technical details and some further results for simulations of SM can be found in the review article by Di Tolla et al. [25].

4. Ionic insulators

Surfaces of ionic crystal such as NaCl, other alkali halides, MgO, etc., are often used as substrates for growing other materials, and their properties are therefore better known far below the melting point than close to it. Yet, some data are also available about their behavior at T_m. In this respect, NaCl appears to be one of the best studied, and can therefore be chosen as a case study. Argon bubble studies of liquid NaCl in contact with the solid revealed a surprising lack of complete wetting, with a large partial wetting angle of about 48 degrees [26]. Very recent MD simulations of solid

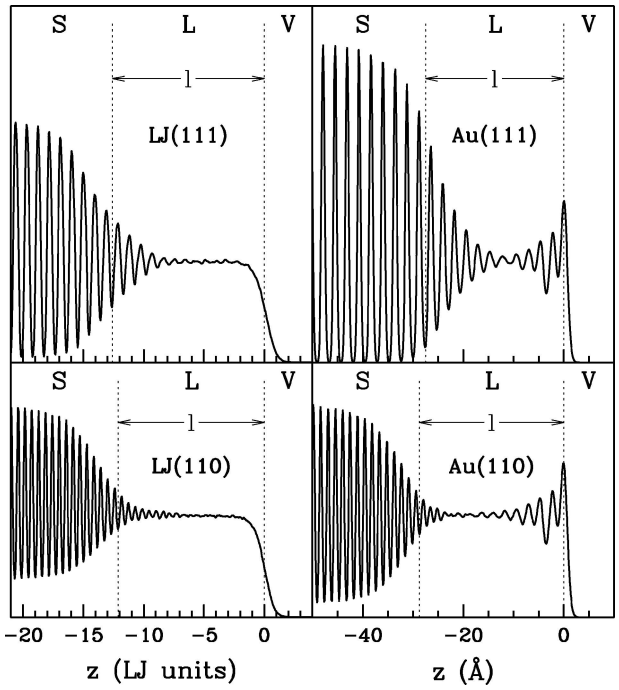

Figure 1 Typical solid-liquid-vapor density profiles obtained by simulations of Lennard-Jones(110) and Au(110) (surfaces that undergo SM) very close to T_m. For Au(111) (which is a NM surface) a nonequilibrium configuration is shown with the oscillations which lead to attraction and eventually to the collapse of the two interfaces (see text). Picture from Ref. [25].

NaCl(100) clearly demonstrate that this partial wetting is related to NM of this solid surface, even predicted to survive in a metastable state well above T_m [27]. Simulations of a droplet of melted NaCl brought into contact with solid NaCl(100) at $T = T_m$ (Fig. 2) demonstrates the incomplete wetting, with an external partial wetting angle of $(50 \pm 5)^\circ$, in good agreement with the bubble experiments [6]. The microscopic reasons for the lack of tendency of solid NaCl(100) to wet itself with molten NaCl are presently under scrutiny.

5. Metals

The surface melting behavior of metallic surfaces has received a great deal of experimental attention. Metal surfaces usually possess positive Hamaker constants, and generally melt. In detail, they may exhibit either melting and nonmelting, depending on the metal and on the crystallographic orientation. A minority of close packed surfaces such as Pb(111) [3], Al(111) and Al(100) [28] displays NM, and in fact remains smooth and dry all the way to T_m. The vast majority of metal faces with all other orientations, where packing is poorer, undergoes SM. In intermediate packing cases like for instance Pb(100) [1], the first few layers melt, but the wetting does not proceed and the liquid film growth is blocked to a finite thickness until T_m (incomplete SM). Although this incomplete melting will appear macroscopically indistinguishable from NM (namely partial wetting with a finite wetting angle), there is a clear microscopic difference because the surface is no longer dry below T_m. An early review of metal surface melting can be found elsewhere [29]. We will limit ourselves here to mention a few hot metal surface phenomena, particularly those connected with NM, which have been especially highlighted in our group.

The first is the existence in surface NM of a critical liquid nucleation thickness ℓ_c which is finite above T_m and only vanishes at some *surface spinodal temperature* $T_s > T_m$. This fact, first discovered in simulation [2], indicates that in NM the solid surface can survive in a metastable state where it is protected by a nucleation barrier, between T_m and T_s. An immediate consequence is that NM solid surfaces can be *overheated*, of course only for a short time, up to at most $T_s > T_m$. For the (111) surfaces of Pb, Al and Au the calculated amount

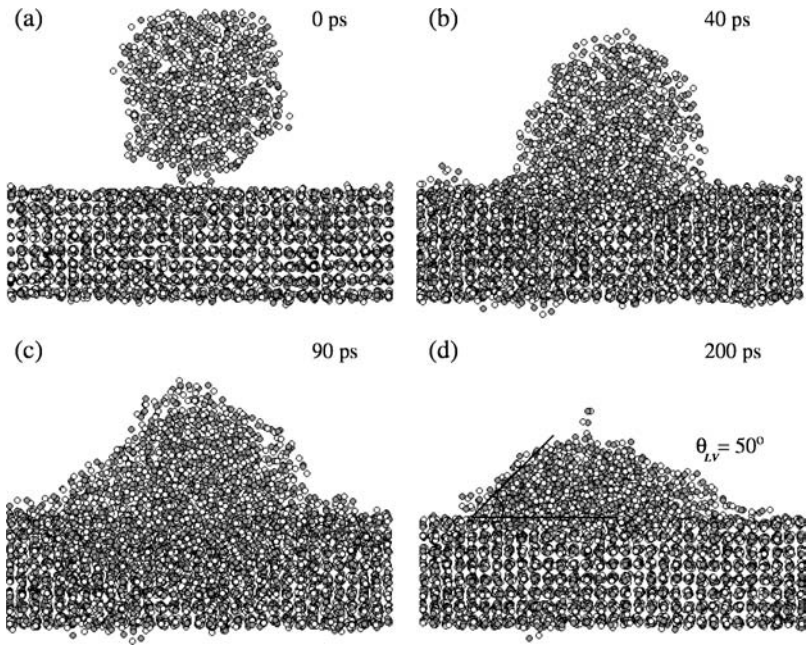

Figure 2 The time evolution of a NaCl liquid droplet brought into the contact with NaCl(100) at the melting point. After 100 ps the drop stabilizes in a metastable state forming a partial wetting contact angle $\theta_{LV} = (50 \pm 5)^\circ$.

of maximum theoretical surface overheating is 120 K, 150 K, and about 150 K respectively. The reality of this possibility was demonstrated experimentally by laser heating techniques [30], and also in small Pb clusters [31].

Another phenomenon discovered theoretically is non-melting induced surface faceting. Consider a general crystal surface, whose orientation is close to, but not exactly coincident with, a flat NM face. Such a *vicinal surface* will consist of a sequence of flat terraces separated by surface steps. At low temperature the steps usually repel and form an ordered array, so that the solid vicinal surface is stable. As T_m is approached, the steps suddenly coalesce in bunches giving way to much larger flat terraces, separated by very inclined facets where the steps have bunched up. The inclined, high-step density facets actually wet themselves, while the step-free flat facets remain dry. This non-melting induced surface faceting—a form of phase separation—was predicted on thermodynamical bases by Noziéres [32], independently demonstrated by MD simulation [33], and eventually observed experimentally [34]. It is most likely the reason why e.g., beautifully perfect flat faces can be generated in gold, by simple heating close to the melting point. Au(111) being a nonmelting face, it will at high temperature require all steps and imperfections to bunch up together someplace, sweeping itself clean and flat.

A further interesting point is the microscopic investigation and clarification of the relationship between solid surface NM and its partial wetting by a drop of melt. While macroscopic partial wetting with a nonzero contact angle of the liquid with its own solid is not commonly reported for metals, it was very clearly found in MD simulation. Ref. [5] shows simulated Al liquid droplet forming the nanoscopic equivalent of a partial wetting angle $\theta_{LV} = (22 \pm 3)^\circ$ in a metastable conditions at $T = 1.01\, T_m$. With the help of a simple model, based on Equation 1 and of a generalized Young equation [5, 32] it was shown that there is a direct relationship between θ_{LV} and the maximum overheating temperature of a NM surface. Using the the calculated ideal overheating temperatures of Pb(111), Al(111) and Au(111) given earlier above, the model predicted partial self-wetting angles θ_{LV} of $(16 \pm 1)^\circ$, $(18 \pm 2)^\circ$, $(33 \pm 2)^\circ$ respectively, in good agreement with the simulation result for Al(111), and with experiments on Pb(111) showing θ_{LV} to be $(14 \pm 1)^\circ$ [34].

Theory and simulation brought out a simple microscopic understanding also for the physics that underlies NM of close packed metal surfaces, based on the intrinsic atomic structure of the SL and LV interfaces [35]. A series of z-resolved in-plane averaged density profiles of the SL and LV interfaces as obtained by MD simulations of Au(111), Au(110), LJ(111) and LJ(111) near T_m is shown in Fig. 1. A damped density oscillation is seen to propagate from the solid into the liquid, carrying approximately the solid interplanar distance as a wavelength. That wavelength of course depends on the crystallographic direction. A second damped density oscillation starts at the liquid surface, carrying *inwards* a different wavelength, determined this time by the main peak in the liquid structure factor $S(k)$. This second oscillation, essentially non-existent in the LJ liquid, is strong in metals, where the surface elicits a stronger density response in the underlying liquid (see further below). Being a property of the liquid, the surface layering oscillation of the surface melted film is face independent. When, as in Au(110), the solid and liquid oscillations facing one another possess wavelengths that are out of tune, their superposition is unfavorable and causes interface repulsion, eventually leading to SM. When instead, as in Au(111), the two oscillations are close to perfectly tuned, their superposition is favorable and causes interface attraction, leading to NM. Finally, the practical absence of a layering oscillation in the LJ liquid surface indicates indifference of the two interfaces. They nonetheless eventually repel via the positive Hamaker constant, and therefore SM ensues in that case too.

6. Special case: Strained solids

In an infinite bulk solid, an increase of hydrostatic pressure generally increases the melting temperature. Contrary to that, uniaxial strain always works the other way around and favors melting, irrespective of the sign of strain. Uniaxial compression or stretching in fact increases the elastic energy of the solid (so long as the solid can sustain the corresponding stress without relevant plastic deformation). On the other hand the liquid does not support shear, all elastic energy released by flow. The bulk melting temperature of a strained solid is thus lowered by an amount which is quadratic in the anisotropic strain. This effect is experimentally observed in He crystals [36]. In metals it has been addressed first through simple thermodynamics, and accessed directly by strained molecular dynamics simulations [37] for Al [38]. A consequence of some practical importance is that in any study of surface melting the strain conditions must be severely controlled. The Al test case indicates that a strain of 10^{-3} implies a shift of T_m of 0.03 K, or 0.003%. As such a degree of precision is sometimes approached in surface melting studies, the error introduced by strains can be significant. Since strain conditions are seldom specified explicitly, it seems possible and in some cases likely that some of the asymptotic SM data in the literature might need re-checking against that source of error. In addition to a lowering of T_m, a strain induced prewetting can also occur. In fact the SV interface will generally possess, in full equilibrium, a nonvanishing surface stress which, when an in-plane bulk strain is applied, will work along with or against the strain, and decrease or increase respectively the overall SV surface free energy γ_{SV}. As seen from Equation 1, an increase of γ_{SV} will further encourage SM, while a decrease will oppose it. In the latter case it can be shown that strain will cause ordinary, continuous SM to be replaced by a *prewetting transition*: as T grows surface melting ceases to be continuous, and develops a sudden jump in the liquid film thickness ℓ from zero to a finite value, from where it then grows continuously and diverges at $T \to T_m$ as in regular SM [38]. This strain-induced prewetting transition has

recently been confirmed by simulations [38], but has yet to be verified experimentally.

7. Liquid metal surfaces

We focused so far on melting of solid surfaces, but *liquid* metal surfaces *per se* have also long been known to be interesting and structured. As revealed by e.g. X-ray reflectivity experiments [39], and as discussed long ago by chemical physicists [40], the density profile of liquid metal surfaces shows a tendency to layering (as also shown by the simulation results of Fig. 1). As said earlier, layering represents the density response of the liquid to vacuum. It is well known that when an external perturbation, say a δ-function point-like repulsion, is inserted into a liquid, the density will locally drop, and will recover away from the point with a damped oscillation dictated by the structure factor $S(k)$, with a wavelength close to $\lambda = 2\pi/k_0$ where k_0 is the position of the first peak of $S(k)$. The surface represents another perturbation of that type (now extended) for the liquid metal, and layering is the result. Layering may lead to high planar density in the liquid surface, as the metal atoms in the outermost surface layer are roughly speaking confined in two dimensions. Moreover, in some cases—like in the heavy noble metals that show a propensity to surface reconstructions—the packing of surface atoms will tend to be closer and tighter than the corresponding bulk atoms. The question therefore arises whether the outer surface of a liquid metal could in some cases go as far as crystallizing in two dimensions (2D). Such a crystallization would represent a case of *surface freezing* —the opposite of surface melting—a phenomenon demonstrated and characterized in alkanes [41]. In two dimensions, freezing should take place in two steps [42]. Disclination pairs should bind into dislocations with a first transition, implying the onset of a *hexatic phase* with power law orientational order. Upon further cooling, a second transition binds dislocation pairs, with the onset of power law positional order. These phenomena are well documented in the melting of 2D colloidal crystal [43]. A liquid metal surface too might be able to exhibit, either above T_m or in the supercooled state, hexatic phase. Floating on a three dimensional liquid, such a phase would be able to exchange freely atoms with it, and disclinations/dislocations could readily form and dissolve avoiding all the delicate kinetic problems presented by strict 2D systems.

Celestini *et al.* [44] carried out MD simulations of the liquid Au surface as a function of temperature particularly in the supercooling regime. As shown by Fig. 3, an increasingly strong layering was indeed found, and the top layer strongly resembling a 2D close packed lattice with a large number of disclinations. Upon supercooling, disclinations rarefied and the system approached a hexatic transition. On the brink of that transition however, bulk crystallization suddenly took place, starting from the liquid surface and moving inwards, and preempting an actual hexatic transition [45]. Further experimental characterization of this type phenomena would seem very desirable.

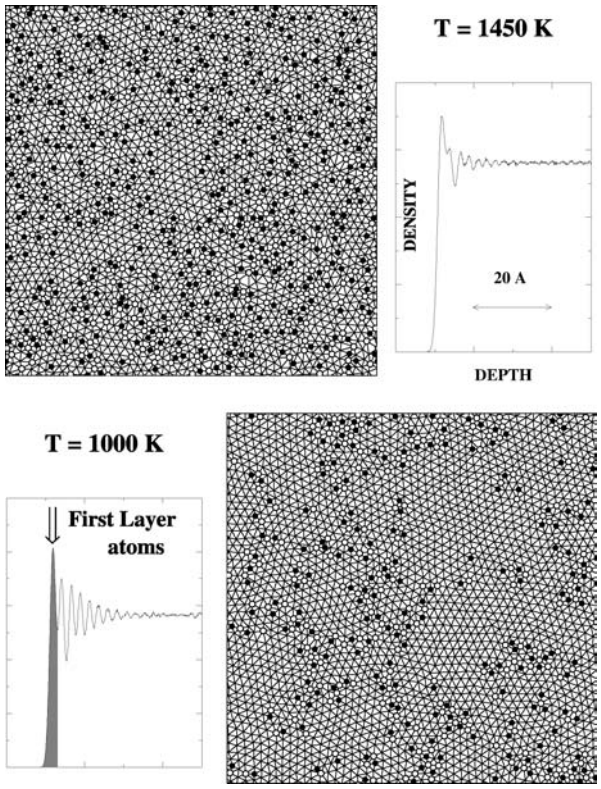

Figure 3 Nearly hexatic top layer of simulated liquid Au [45], both above and below (undercooling) the melting point $T_m = 1335$ K. Fivefold (black) and sevenfold (white) disclinations are pinpointed. The corresponding density profiles along the surface normal are also shown. The first peak corresponds to the outmost layer of atoms in the maps.

8. Premelting of nanoclusters and nanowires

As has long been known, small clusters readily liquefy, or *premelt*, well below the bulk melting temperature T_m of the same material. Basic thermodynamics predicts phenomenologically that a cluster of radius R should melt at $T_m(R) \simeq T_m^\infty(1-C/R)$, where the coefficient C is approximatively proportional to $\gamma_{SV} - \gamma_{LV}$, and T_m^∞ is the bulk melting temperature. The lowering of T_m is driven by the difference in the surface free energy between liquid and solid. This behavior was well verified experimentally in Au by classic cluster beam experiments by Buffat and Borel [46]. A similar melting behavior (with a different C) is expected for one-dimensional extended nanosystems, such as nanowires [47].

Microscopic theories as well as atomistic MD simulations of cluster melting are numerous and well documented. A review can be found in standard books [48, 49]. Fig. 4, obtained by MD simulations [50], shows that in the case of Pb clusters the melting temperature indeed decreases linearly with the inverse radius. For Au clusters, of special experimental interest and more complex due to surface reconstructions, we carried out MD simulations in order to understand how the premelted state was reached for increasing temperature [51]. The $1/R$ decrease for T_m was confirmed, and it was found that (unless the cluster is so small to melt at $T_m^\infty/2$ or below) liquid-like diffusivity sets up at the surface below the melting temperature. Melting at $T_m(R)$ occurs by a sudden propagation of this liquid "skin" into the bulk-like interior. This behavior is quite

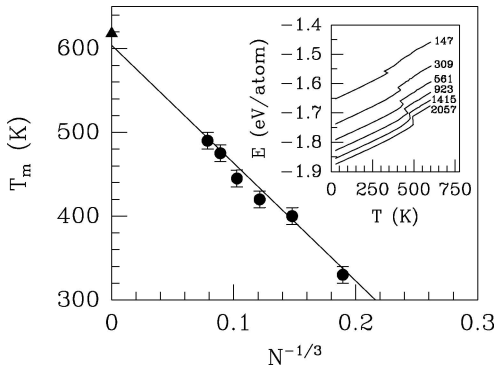

Figure 4 Melting temperature as a function of $N^{-1/3}$ (where N is the number of atoms) of simulated Pb clusters. The points correspond to the discontinuities in the caloric curves in the inset. The solid line is a linear fit to the points. The triangle corresponds to bulk melting.

similar to that described by a phenomenological model of Celestini *et al.* [52].

One would expect that clusters entirely bounded by NM crystal faces do not premelt. While that has been confirmed in Pb clusters [53], it is not generally true. For example, clusters of systems such as In [54] have been shown to premelt, despite the nonmelting nature of In faces, where $H < 0$. The problem is that macroscopic reasoning ignores microscopic details, such as edges and corners, features that the clusters nonetheless possess. The simulated high temperature behavior of a NaCl cubic nanocluster (a *nanograin of salt*) is in that respect quite revealing [6]. The (100) nanocube faces are NM: if they were unbounded, there would indeed be no premelting. However the cube corners are the weak spot, and begin melting even below T_m. While NaCl corner roughening was described long ago [55] it did not necessarily imply melting. In our realistic simulations [6] the edges not only round but liquefy, and the melting front does not stop at corners, but readily sweeps through the small cluster which premelts.

It is in principle an open question how the picture should evolve with increasing grain size. Clearly the corners will represent in all cases point-like germs of the liquid which are present below T_m. While these germs will certainly enlarge into liquid pools, it remains to be clarified how the pools will spread out, and if and in what form their presence will permit, if at all, the faces of a large NaCl cube to exhibit NM, and to remain solid up to and above T_m. More generally, this approach would probably shed light also on the premelting of nanoparticles made of $H < 0$ mentioned above.

Acknowledgments

This project was sponsored by Italian Ministry of University and Research, through COFIN03, COFIN04 (Nanotribologia), FIRB RBAU01LX5H, and FIRB RBAU017S8R; and by INFM, through PRA NANORUB and "Iniziativa Trasversale calcolo parallelo". A large fraction of the calculations were performed at CINECA, Casalecchio (Bologna).

References

1. J. W. M. FRENKEN, P. M. J. MAREE and J. F. VAN DER VEEN, *Phys. Rev. B* **34** (1986) 7506.
2. P. CARNEVALI, F. ERCOLESSI and E. TOSATTI, *ibid.* **36** (1987) 6701.
3. B. PLUIS, A. W. DENIER VAN DER GON, J. W. M. FRENKEN and J. F. VAN DER VEEN, *Phys. Rev. Lett.* **59** (1987) 2678.
4. L. D. LANDAU and E. M. LIFSHITZ, "Statistical Physics" (Pergamon, 1980) Ch. XV.
5. F. D. DI TOLLA, F. ERCOLESSI and E. TOSATTI, *Phys. Rev. Lett.* **74** (1995) 3201.
6. T. ZYKOVA-TIMAN, U. TARTAGLINO, D. CERESOLI and E. TOSATTI, to be published.
7. B. PLUIS, T. N. TAYLOR, D. FRENKEL and J. F. VAN DER VEEN, *Phys. Rev. B* **40** (1989) 1353.
8. J. N. ISRAELACHVILI, "Intermolecular and Surface Forces" (Academic Press, San Diego, 1985).
9. J. G. DASH *Contemp. Phys.* **30** (1989) 89; J. G. DASH, *Rep. Prog. Phys.* **58** (1995) 115.
10. U. TARTAGLINO, T. ZYKOVA-TIMAN, F. ERCOLESSI and E. TOSATTI, *Phys. Rep.*, in press.
11. P. M. PLATZMAN and H. FUKUYAMA, *Phys. Rev. B* **10** (1974) 3150.
12. L. PIETRONERO and E. TOSATTI, *Solid State Commun.* **32** (1979) 255.
13. G. TAMMANN, *Z. Phys. Chem.* **68** (1910) 205; I. N. STRANSKI, *Z. Phys.* **119** (1942) 22; D. Nenow,"Progress in crystal growth and characterization" (pergamon, Oxford, 1984) Vol. 9, p. 185.
14. C. S. JAYANTHI, E. TOSATTI and A. FASOLINO, *Phys. Rev. B* **31** (1985) 470; C. S. Jayanthi, E. TOSATTI and L. PIETRONERO, *ibid.* **31** (1985) 3456.
15. A. M. MOLENBROEK and J. W. M. FRENKEN, *ibid.* **50** (1994) 11132.
16. A. TRAYANOV and E. TOSATTI, *Phys. Rev. Lett.* **59** (1987) 2207; *Phys. Rev. B* **38** (1988) 6961.
17. R. LIPOWSKY and W. SPETH, *Phys. Rev. B* **28** (1983) 3983.
18. A. A. CHERNOV and L. V. MIKHEEV, *Phys. Rev. Lett.* **60** (1988) 2488; *Physica A* **157** (1982) 1042.
19. M. S. DAW and M. I. BASKES, *Phys. Rev. B* **29** (1984) 6443.
20. F. ERCOLESSI, M. PARRINELLO and E. TOSATTI, *Phil. Mag. A* **58** (1988) 213.
21. M. W. FINNIS and J. E. SINCLAIR, *Phil. Mag. A* **50** (1984) 45; *Phil. Mag. A* **53**(Erratum), (1986) 161.
22. D. W. BRENNER, *Phys. Rev. B* **42** (1990) 9458.
23. J. TERSOFF, *ibid.* **37** (1988) 6991.
24. N. TAKEUCHI, A. SELLONI and E. TOSATTI, *Phys. Rev. Lett.* **72** (1994) 2227.
25. F. DI TOLLA, E. TOSATTI and F. ERCOLESSI, in "Monte Carlo and Molecular Dynamics of Condensed Matter Systems" edited by K. Binder and G. Ciccotti (Società Italiana di Fisica, Bologna, 1996) p. 345.
26. G. GRANGE and B. MUTAFTSCHIEV, *Surf. Sci.* **47** (1975) 723.
27. T. ZYKOVA-TIMAN, U. TARTAGLINO, D. CERESOLI, W. ZAOUI-SEKKAL and E. TOSATTI, *Surf. Sci.* **566–568** (2004) 794.
28. A. M. MOLENBROEK and J. W. FRENKEN, *Phys. Rev. B* **50** (1994) 11132; A. M. MORENBROEK, Ph.D. thesis, Univ. of Amsterdam (1995).
29. J. F. VAN DER VEEN, in "Phase Transitions in Surface Films 2", edited by H. Taub *et al.* (NATO – ASI Series B, New York, 1991) Vol. 267, p. 289.
30. J. W. HERMAN and H. E. ELSAYED-ALI, *Phys. Rev. Lett.* **74** (1995) 3201.
31. J. J. MÉTOIS and J. C. HEYRAUD, *J. Phys. (France)* **50** (1989) 3175.
32. P. NOZIÉRES, *ibid.* **50** (1989) 2541.
33. G. BILALBEGOVIĆ, F. ERCOLESSI and E. TOSATTI, *Europhys. Lett.* **17** (1992) 333.
34. H. M. VAN PINXTEREN, B. PLUIS and J. W. M. FRENKEN, *Phys. Rev. B* **49** (1994) 13798.
35. O. TOMAGNINI, F. ERCOLESSI, S. IARLORI, F. D. DI TOLLA and E. TOSATTI, *Phys. Rev. Lett.* **76** (1996) 1118.
36. R. H. TORII and S. BALIBAR, *Physica B* **194** (1994) 971.

37. D. PASSERONE, E. TOSATTI, G. L. CHIAROTTI and F. ERCOLESSI, *Phys. Rev. B* **59** (1999) 7687.
38. U. TARTAGLINO, E. TOSATTI, *Surf. Sci.* **532** (2003) 623.
39. see, e.g., H. TOSTMANN, E. DIMASI, P. S. PERSHAN, B. M. OCKO, O. G. SHPYRKO and M. DEUTSCH, *Phys. Rev. B* **61** (2000) 7284.
40. H. L. LEMBERG, S. A. RICE and D. GUIDOTTI, *ibid.* **10** (1974) 4079.
41. X. Z. WU, E. B. SIROTA, S. K. SINHA, B. M. OCKO and M. DEUTSCH, *Phys. Rev. Lett.* **70** (1993) 958; X. Z. WU, B. M. OCKO, E. B. SIROTA, S. K. SINHA, M. DEUTSCH, B. M. CAO and M. W. KIM, *Science* **261** (1993) 1018.
42. D. R. NELSON and B. I. HALPERIN, *Phys. Rev. Lett.* **41** (1978) 121.
43. C. A. MURRAY and R. A. WENK, *ibid* **62** (1989) 1643.
44. D. PASSERONE, F. ERCOLESSI, F. CELESTINI and E. TOSATTI, *Surf. Rev. Lett.* **6** (1999) 663.
45. F. CELESTINI, F. ERCOLESSI and E. TOSATTI, *Phys. Rev. Lett.* **78** (1997) 3153.
46. PH. BUFFAT and J. P. BOREL, *Phys. Rev. A* **13** (1976) 2287.
47. O. GÜLSEREN, F. ERCOLESSI and E. TOSATTI, *Phys. Rev. B* **51** (1995) 7377.
48. K. S. LIANG, M. P. ANDERSON, R. F. BRUINSMA and G. SCOLES, "Interface Dynamics and Growth" (Pa.(MRS), Pittsburgh, 1992).
49. V. KUMAR, T. P. MARTIN and E. TOSATTI, Clusters and Fullerenes: Proceedings of the Adriatico Research Conference, Trieste, Italy, June 23–26, 1992 (World Scientific, Singapore, 1993).
50. H. S. LIM, C. K. ONG and F. ERCOLESSI, *Zeitschrift fur Physik* **26** (1993) S45.
51. F. ERCOLESSI, W. ANDREONI and E. TOSATTI, *Phys. Rev. Lett.* **66** (1991) 911.
52. F. CELESTINI and A. TEN BOSCH, *Phys. Lett. A* **207** (1995) 307.
53. J. J. MÉTOIS and J. C. HEYRAUD, *J. Microsc. Spect. Elec.* **14** (1989) 343.
54. A. PAVLOVSKA, D. DOBREV and E. BAUER, *Surf. Sci.* **286** (1993) 176.
55. M. WORTIS, in "Chemistry and Physics of Solid Surfaces VIII", edited by R. Vanselow and R. Howe (Springer-Verlag, Berlin, 1990).

Received 31 March
and accepted 18 July 2004